A Multiplexed Quantum Memory

S.-Y. Lan[1], A. G. Radnaev[1], O. A. Collins[1], D. N. Matsukevich[2], T. A. B. Kennedy[1] and A. Kuzmich[1]

[1]*School of Physics, Georgia Institute of Technology, Atlanta, Georgia 30332-0430*
[2]*Department of Physics, University of Maryland, College Park, Maryland 20742*
alex.kuzmich@physics.gatech.edu

Abstract: A quantum repeater is a system for long-distance quantum communication that employs quantum memory elements to mitigate optical fiber transmission losses. The multiplexed quantum memory (O. A. Collins, S. D. Jenkins, A. Kuzmich, and T. A. B. Kennedy, Phys. Rev. Lett. **98**, 060502 (2007)) has been shown theoretically to reduce quantum memory time requirements. We present an initial implementation of a multiplexed quantum memory element in a cold rubidium gas. We show that it is possible to create atomic excitations in arbitrary memory element pairs and demonstrate the violation of Bell's inequality for light fields generated during the write and read processes.

OCIS codes: (020.0020) Atomic and molecular physics; (270.5565) Quantum communications; (270.5568) Quantum cryptography.

References and links

1. W. Duer, H. J. Briegel, , I. J. Cirac, and P. Zoller, "Quantum repeaters based on entanglement purification," Phys. Rev. A **59**, 169-181 (1999).
2. L.-M. Duan, M. Lukin, M., I. J. Cirac, and P. Zoller, "Long-distance quantum communication with atomic ensembles and linear optics," Nature **414**, 413-418 (2001).
3. H. J. Briegel, W. Duer, H. J., I. J. Cirac, and P. Zoller, "Quantum repeaters: The role of imperfect local operations in quantum communication," Phys. Rev. Lett. **81**, 5932-5935 (1998).
4. O. A. Collins, S. D. Jenkins, A. Kuzmich, and T. A. B. Kennedy, "Multiplexed memory-insensitive quantum repeaters," Phys. Rev. Lett. **98**, 060502 (2007).
5. N. Sangouard, C. Simon, B. Zhao, Y. A. Chen, H. de Riedmatten, J. W. Pan, and N. Gisin, "Robust and efficient quantum repeaters with atomic ensembles and linear optics," Phys. Rev. A **77**, 062301 (2008).
6. L. Jiang, J. M. Taylor, and M. D. Lukin, "Fast and robust approach to long-distance quantum communication with atomic ensembles," Phys. Rev. A **76**, 012301 (2007).
7. D. N. Matsukevich, and A. Kuzmich, "Quantum state transfer between matter and light," Science **306**, 663-666 (2004).
8. T. Chanelière, D. N. Matsukevich, S. D. Jenkins, S.-Y. Lan, T. A. B. Kennedy, and A. Kuzmich, "Quantum telecommunication based on atomic cascade transitions," Phys. Rev. Lett. **96**, 093604 (2006).
9. D. N. Matsukevich, T. Chanelière, S. D. Jenkins, S.-Y. Lan, T. A. B. Kennedy, and A. Kuzmich, "Deterministic single photons via conditional quantum evolution," Phys. Rev. Lett. **97**, 013601 (2006).
10. T. Chanelière, D. N. Matsukevich, S. D. Jenkins, S.-Y. Lan, T. A. B. Kennedy, and A. Kuzmich, "Storage and retrieval of single photons transmitted between remote quantum memories," *Nature* **438**, 833-836 (2005), and Supplementary Online Information.
11. D. N. Matsukevich, T. Chanelière, S. D. Jenkins, S.-Y. Lan, T. A. B. Kennedy, and A. Kuzmich, "Observation of collapses and revivals collapses and revivals," Phys. Rev. Lett. **96**, 033601 (2006).
12. D. N. Matsukevich, T. Chanelière, S. D. Jenkins, S.-Y. Lan, T. A. B. Kennedy, and A. Kuzmich, "Entanglement of remote atomic qubits," Phys. Rev. Lett. **96**, 030405 (2006).
13. S. D. Jenkins, D. N. Matsukevich, T. Chanelière, A. Kuzmich, and T. A. B. Kennedy, Theory of dark-state polariton collapses and revivals," Phys. Rev. A **73**, 021803(R) (2006).
14. J. Simon, H. Tanji, S. Ghosh, and V. Vuletic, "Single-photon bus connecting spin-wave quantum memories," Nature Phys. **3** 765-769 (2007).

#112719 - $15.00 USD Received 11 Jun 2009; revised 10 Jul 2009; accepted 20 Jul 2009; published 23 Jul 2009

15. S.-Y. Lan, D. N. Matsukevich, T. Chanelière, S. D. Jenkins, T. A. B. Kennedy, and A. Kuzmich, "Dual species matter qubit entangled with light," Phys. Rev. Lett. **98**, 123602 (2007).
16. Y. A. Chen, S. Chen, Z. S. Yuan, B. Zhao, C. S. Chuu, J. Schmiedmayer, and J. W. Pan, "Memory-built-in quantum teleportation with photonic and atomic qubits," Nature Phys. **4**, 103-107 (2008).
17. K. S. Choi, H. Deng, J. Laurat, and H. J. Kimble, "Mapping photonic entanglement into and out of a quantum memory," Nature **452**, 67-74 (2008).
18. R. Zhao, Y. O. Dudin, S. D. Jenkins, C. J. Campbell, D. N. Matsukevich, T. A. B. Kennedy, and A. Kuzmich, "Long-lived quantum memory," Nature Phys. **5**, 100-104 (2009).
19. Y. O. Dudin, S. D. Jenkins, R. Zhao, D. N. Matsukevich, A. Kuzmich, and T. A. B. Kennedy, "Entanglement of a photon and an optical lattice spin wave," Phys. Rev. Lett. **103**, 020505 (2009).
20. J. S. Bell, "On the Einstein-Podolsky-Rosen paradox," Physics **1**, 195-200 (1964).
21. J. S. Bell, "On the problem of hidden variables in quantum mechanics," Rev. Mod. Phys. **38**, 447 - 452 (1966).
22. J. F. Clauser, M. A. Horne, A. Shimony, and R. A. Holt, "Proposed experiment to test local hidden-variable theories," Phys. Rev. Lett. **23**, 880-884 (1969).
23. B. Zhao, Z.-B. Chen, Y.-A. Chen, J. Schmiedmayer, and J.-W. Pan, "Robust creation of entanglement between remote memory qubits," Phys. Rev. Lett. **98**, 240502 (2007).

Quantum communication seeks to use entanglement to securely transmit information between remote locations. Distribution of entanglement over continental-scale optical fiber networks will require methods to mitigate fiber loss. Quantum repeater architectures, which use quantum memory elements as nodes and telecommunication wavelength light for transmission, hold promise to achieve such long-distance communication [1, 2, 3, 4, 5, 6].

In a seminal paper Duan *et al.* have proposed to use atomic ensembles as the memory elements of the quantum repeater [2]. Following this work advances in the interface of single photon fields and alkali atom memories have been made [7, 8, 9, 10, 11, 12, 13, 14, 15, 16, 17, 18]. The protocols proposed to distribute entanglement over large distances require quantum memory storage lifetimes that are large compared to the classical communication time between nodes. Storage lifetime requirements are increased further by the actual communication process. Over a single network segment, multiple successful entanglement distributions are necessary within the quantum memory lifetime, for the formation of a single quantum bit. Recently quantum memory lifetimes in excess of 6 ms have been demonstrated [18, 19]. Quantum network protocols indicate that for communication over distances of 1,000 km, quantum memory lifetimes of many seconds are required, and the memory should be compatible with telecom wavelength light to minimize fiber transmission losses. Demonstration of long-lived quantum memory qubits entangled with telecommunication wavelength light fields remains an outstanding challenge. In atomic ensembles, cascade emission rather than Raman scattering, which produces shorter wavelength infrared light, has been suggested as a method of generating the telecom wavelength photons [8].

One could significantly increase the rate of entanglement distribution for much shorter memory lifetimes by placing many memory elements at each node and dynamically reconfiguring the connections between them, thereby increasing the number of repeater states where entanglement distribution is possible. This multiplexed repeater protocol greatly improves entanglement distribution rates, which in turn produce even more dramatic improvements in quantum communication rates. Multiplexed quantum memory arrays boost communication rates by orders of magnitude, with significantly shorter memory lifetime requirements [4].

We report the first demonstration of a quantum memory element array, by spatially dividing a gas of cold Rubidium atoms into 12 independently addressable memory elements. Having established conditions that the elements operate independently to a sufficient degree, we show that arbitrary element pairs can be coherently addressed, generating matter-light entanglement. Our demonstration employs Raman scattering which generates photons in the near-infrared region. However, the benefits of multiplexing to future quantum repeater operation will be relevant only when both telecom wavelength light and millisecond or longer quantum memory

#112719 - $15.00 USD Received 11 Jun 2009; revised 10 Jul 2009; accepted 20 Jul 2009; published 23 Jul 2009

lifetimes are employed together.

In a practical setting the memory elements would be repeatedly addressed, by a sequence of laser pulses, in order to generate and distribute entanglement according to a probabilistic protocol [2, 4, 5, 6]. The pulse sequence begins with a weak *write* laser field which attempts to generate an atomic spin-wave excitation, heralded by detection of a Raman scattered signal photon. In the absence of photoelectric detection the write field is followed by a strong clean pulse which removes unheralded atomic excitations and returns atoms to their initial ground hyperfine level.

Retrieval is achieved by a *read* laser which converts the matter excitation into an idler field, Fig. 1. The quantum correlations between idler and signal fields are strong under conditions of four-wave mixing, with respect to the write, read, signal and idler field wave vectors. It is essential to ensure the array elements operate independently, and that attempts to excite a given memory element do not cause excitation of its neighbours. Here we quantify the degree of independence by measurements of the retrieval efficiency, $\eta^{(k)}$, of element k when its nearest neighbors are subjected to a write-clean trial sequence. The latter should ideally have no effect on $\eta^{(k)}$, whereas there is an observed reduction in the retrieval efficiency depending on the element separation and other system parameters.

The quantum memory array is illustrated in Fig. 1. It is produced by dividing a cold cloud of ^{85}Rb atoms (prepared in a MOT of diameter 2.6 mm and temperature $T \simeq 100\ \mu$K) into separate elements. These are addressed by frequency controlled deflection of laser beams using four AODs with a 50 MHz central frequency and RF bandwidth (full width half maximum) Δf = 30 MHz, so that element $j = 1,..,12$ is addressed with RF field of frequency $f_j = (36+1.8j)$ MHz. These AODs also serve as dynamic phase-controlled beamsplitters, enabling the generation and verification of matter-light entanglement for an arbitrary pair of memory elements. The waist of the write/read modes is 115(3) μm, while that of the signal and idler fields is 30(6) μm); beam waist is defined as the half-width at $1/e^2$ of maximum intensity.

The maximum number of elements in a linear array based on light beam scanning is given by $\theta D/\lambda$ where θ and $D = 0.3$ mm are the angular range and aperture diameter of the scanning element and $\lambda = 795$ nm is the wavelength of light. For an AOD, $\theta = \lambda\Delta f/V$, where $V = 660$ m/s is the velocity of sound, so that we may write the number of elements $N \simeq \Delta f \Delta T$, where $\Delta T = D/V \simeq 0.4\ \mu$s is the access time; for the parameters of our experiment, $N \sim 10$.

The protocol begins with atoms prepared in level $|b\rangle$ and released from the trap (the magnetic field, trapping, and repumping light are switched off). In order to create a spin-wave excitation in one of the elements, a sequence of 250 ns long write laser pulses of 3 μW power, separated by 1.3 μs, illuminate the memory array, one pulse per element (see Fig. 1). The write field is red-detuned by 10 MHz. The signal AOD is synchronously driven to direct the scattered signal field onto a single mode collection fiber coupled to a photoelectric detector. If a signal field photoelectric event is not detected a 100 ns long clean pulse of 10 μW power, resonant with the $|a\rangle - |c\rangle$ transition returns the atoms to level $|b\rangle$. Once a signal photodetection event is recorded, the write process is stopped, and the FPGA measures the time of this event with a resolution of 5 ns. After a further 10 μs delay, the spin-wave excitation is converted to the idler field using a 200 ns long read laser pulse of 500 μW power. An idler field photoelectric detection event terminates the protocol. This sequence is repeated at a frequency of 6.1 kHz (approximately 100 cycles over a period of 14 ms), and the retrieval efficiencies of each element measured. The retrieval efficiency of element k is defined as the ratio of the number of signal-idler coincidence counts, $C_{si}^{(k)}$, to the number of signal counts, $C_s^{(k)}$, over the data acquisition period, $\eta^{(k)} \equiv C_{si}^{(k)}/C_s^{(k)}$. The central element has the largest retrieval efficiency, 2.1%, while the array average is 1.1%.

Crosstalk between array memory elements is expected to arise mainly due to the strong clean

#112719 - $15.00 USD Received 11 Jun 2009; revised 10 Jul 2009; accepted 20 Jul 2009; published 23 Jul 2009

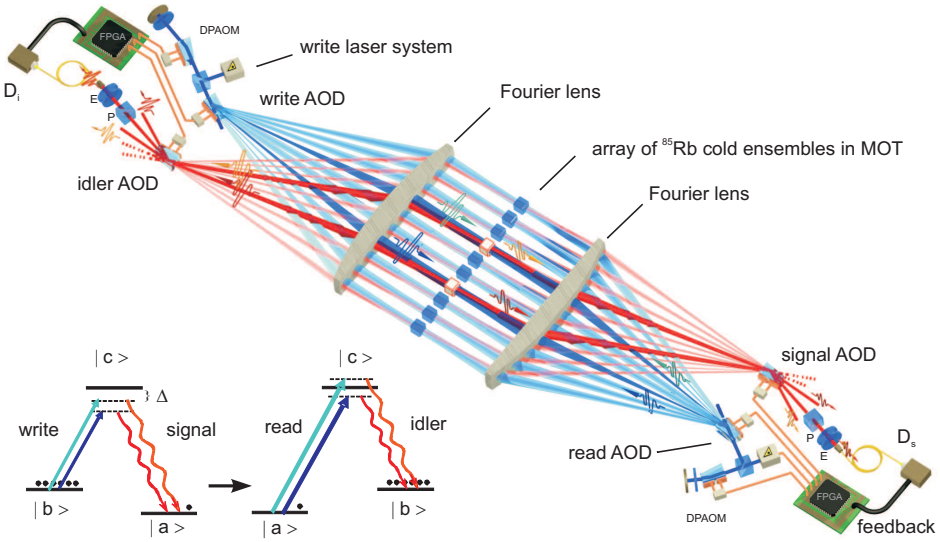

Fig. 1. Schematic illustration of the quantum memory array, for clarity showing 10 rather than 12 elements. A cold sample of ^{85}Rb atoms is produced in a magneto-optical trap (MOT). The atoms are addressed with laser beams whose position is controlled by an acoust-optic deflector (AOD), followed by a 10 cm focal length Fourier lens, used to map angular deflection into spatial translation. One pair of AODs mode-matches the write and read beams, determining the array element locations, while another pair collects the scattered signal and idler fields which are directed onto single photon detectors (D_s and D_i, respectively) through etalon (E) and polarization filters (P). The signal(write) mode of each element is coupled into the idler(read) fiber mode with about 75% efficiency. The position of the four intersecting beams is controlled by simultaneously varying the AOD drive frequencies by means of a field-programmable gate array (FPGA). The four-wave mixing condition, $\mathbf{k}_w^{(j)} + \mathbf{k}_r^{(j)} = \mathbf{k}_s^{(j)} + \mathbf{k}_i^{(j)}$, is satisfied for each array element j by using telecentric scanning. The write and read light frequency shifts are compensated by additional AOMs in a double-pass configuration (DPAOM). The measured average separation between array elements is 230 μm. The two highlighted elements represent a matter qubit, in which an atomic spin-wave in one of the elements represents logical 0, and in the other logical 1, see text for details. The atomic energy level diagram shows the Raman scattering sequence of write and read laser excitation and retrieval employed in the quantum memory, where $|a\rangle = |5s_{1/2}, F = 2\rangle, |b\rangle = |5s_{1/2}, F = 3\rangle, |c\rangle = |5p_{1/2}, F = 3\rangle$; the write field detuning $\Delta = 10$ MHz.

pulses that are used after every unsuccessful excitation trial to reset the atomic memory element. The degree of crosstalk experienced by a given element can be quantified by perturbing its nearest neighbors prior to read-out, and comparing the read-out efficiency with that measured in the absence of perturbation. Specifically, our perturbation consists of 10 clean pulses sent to each of the two nearest neighbors of the excited element; for edge elements, 20 pulses are sent to the neighbouring element. A clean pulse is simply a time-displaced version of the corresponding read pulse. We extract the average crosstalk $\kappa = \langle \kappa^{(k)} \rangle$ assuming $\eta_p^{(k)} = (1 - \kappa^{(k)})^{20} \eta^{(k)}$, where $\eta^{(k)}$ is the read-out efficiency without perturbation, and $\eta_p^{(k)}$ is the perturbed efficiency, for element k. For 12 elements in a linear array, with element separation d = 230 μm, the measured crosstalk $\kappa = 1.5(6)\%$. The crosstalk could clearly be reduced by increasing d, although in our experiment a substantial contribution comes from RF noise on the AOD driving field.

#112719 - $15.00 USD Received 11 Jun 2009; revised 10 Jul 2009; accepted 20 Jul 2009; published 23 Jul 2009

The crosstalk between different elements due to atomic motion is negligible since the average atomic velocity in the MOT is $v \sim 0.1$ m/s, and the displacement, s, of an atom during a spin-wave storage time of 10 μs is about 1 μm, so that $s << d$.

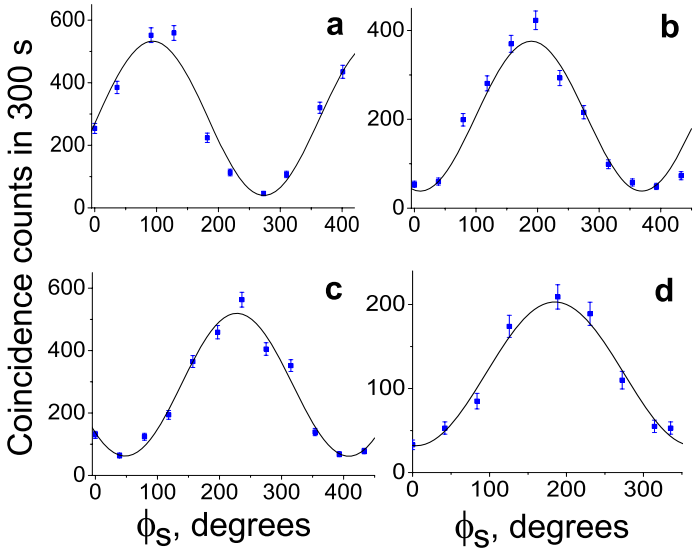

Fig. 2. Measured coincidence fringes as functions of a signal phase ϕ_s, corresponding to array elements (7,8) (a), (5,10) (b), (7,10) (c), and (1,12) (d). Sinusoidal fits give corresponding visibilities 0.86(2), 0.81(2), 0.79(1), 0.73(3). Each data point has acquisition time 5 min. The effective repetition rate is 100 kHz, and each trial takes 1.5 μs. Error bars represent ± 1 standard deviation based on photoelectron counting statistics.

With crosstalk at the level of 1-2% we attempt to create a matter qubit using two arbitrary elements, (j,k), of the array. The matter qubit is ideally entangled with a light qubit, encoded in corresponding spatial modes of the signal field. The matter-light entanglement is investigated by measuring violation of Bell's inequality for the signal and idler fields scattered from elements j,k.

We generate two spatially distinct write pulses by providing the AOD aligned in +1 diffraction order with two different frequencies f_j and f_k corresponding to ensembles j and k. Suppose that $f_j > f_k$, then the write field (red) detuning of element j is smaller than that of element k, and set to the value 10 MHz; the corresponding detuning of element k is given by 10 MHz $+f_j - f_k$. The spatially separated write pulses, of 250 ns duration, illuminate ensembles j and k simultaneously generating the signal field by Raman scattering. The signal field is directed to the signal AOD, aligned in -1 diffraction order and driven by the same RF signal as the write field. As a result the relative phase of the two signal fields is insensitive to the phase drifts of the RF sources. The signal fields traverse the same optical elements and as a result the interferometer is passively stable. To compensate for the dependence of excitation probability on write field frequency, we adjust the corresponding write field intensities.

After a 150 ns delay we convert the element j and k spin-wave excitations to idler fields, with two read pulses of 200 ns duration generated by an AOD aligned in +1 diffraction order and driven by frequencies f_j and f_k as before. The read pulses are detuned by $\pm(f_j - f_k)/2$ from

#112719 - $15.00 USD Received 11 Jun 2009; revised 10 Jul 2009; accepted 20 Jul 2009; published 23 Jul 2009

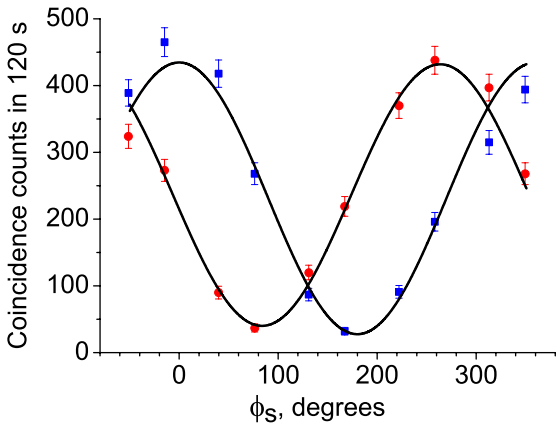

Fig. 3. Measured coincidence fringes corresponding to array elements 5 and 8, as functions of ϕ_s for ϕ_i=0°, squares and ϕ_i= 90°, circles. The solid curves are fits by a function $C_{si}(\phi_s,\phi_i) \propto 1+V\cos(\phi_i+\phi_s+\phi_0)$ with visibilities V =(0.88(2), 0.83(2)) and phase offsets ϕ_0=(0(1)°,5(3)°) for curves with $\phi_i = 0°$ and $\phi_i = 90°$, respectively. Error bars represent ±1 standard deviation based on photoelectron counting statistics.

the $|a\rangle \rightarrow |c\rangle$ transition, for elements j and k, respectively. The detunings are chosen to equalize retrieval efficiencies and their magnitude is determined by the AOD used. We measure the joint signal and idler field photodetection rate $C_{si}^{(j,k)}$ as a function of the signal and idler phase delays ϕ_s and ϕ_i. The latter are varied by adjusting the delay of element k's signal and idler AOD RF driving fields with respect to those of the write and read fields; we assume $f_j > f_k$. We observe the characteristic sinusoidal dependence $C_{si}^{(j,k)}(\phi_s,\phi_i) \propto 1+V^{(j,k)}\cos(\phi_i+\phi_s)$, where $V^{(j,k)}$ is the visibility.

Joint signal-idler detection data are shown for various element pairs in Fig. 2. These show high visibility fringes in all cases, including the (1,12) pair corresponding to the edge elements, where the frequency detuning of write and read fields is largest. To investigate matter-light entanglement we randomly select elements 5 and 8 for further analysis. In Fig. 3 we show the data for $C_{si}^{(5,8)}$ as a function of ϕ_s for $\phi_i = 0$ and $\phi_i = \pi/2$, respectively. It is well known that the visibility can be extracted by combining measurements of $C_{si}^{(j,k)}(\phi_s,\phi_i)$ for particular phase angles, leading to the normalized correlation function $E^{(j,k)}(\phi_i,\phi_s) = V^{(j,k)}\cos(\phi_i+\phi_s)$ [20, 21, 22]. A classical local hidden variable theory yields Bell's inequality $|S| \leq 2$, where the Bell parameter $S \equiv E(\phi_s,\phi_i)+E(\phi_s',\phi_i)-E(\phi_s,\phi_i')+E(\phi_s',\phi_i')$, and we suppress the superscripts j and k. Measured values of the correlation function E using the set of angles $\phi_s = 135°$, $\phi_s' = 45°$, $\phi_i = -90°$, $\phi_i' = 0°$, are listed in Table 1, and lead to violation of Bell's inequality, $|S| = 2.38 \pm 0.03$.

Table 1. **Measured correlation function $E(\phi_s,\phi_i)$ and S for ensemble 5 and 8.**

ϕ_i	ϕ_s	$E(\phi_s,\phi_i)$
$-90°$	$45°$	0.625 ± 0.016
$-90°$	$135°$	0.562 ± 0.017
$0°$	$45°$	0.510 ± 0.018
$0°$	$135°$	-0.683 ± 0.017
		$\lvert S\rvert = 2.38 \pm 0.03$

In addition to dramatically improving quantum repeater performance based on non-local

#112719 - $15.00 USD Received 11 Jun 2009; revised 10 Jul 2009; accepted 20 Jul 2009; published 23 Jul 2009

entanglement generation [2, 4], multiplexed memory elements should also enable local entanglement generation protocols [23, 6]. By employing two-dimensional, broadband, scanning techniques the number of addressable elements could be significantly increased, along with entanglement distribution rates.

This work was supported by the National Science Foundation, Air Force Office of Scientific Research, A. P. Sloan Foundation, and Army Research Office through the Georgia Tech Quantum Institute.

#112719 - $15.00 USD Received 11 Jun 2009; revised 10 Jul 2009; accepted 20 Jul 2009; published 23 Jul 2009